Applied Cellular Physiology and Metabolic Engineering

Biotechnology Progress
DOI 10.1002/btpr.2273

Promoter engineering to optimise recombinant periplasmic Fab' fragment production in *Escherichia coli.*

Desmond M. Schofield, Alex Templar, Joseph Newton, Darren N. Nesbeth*.

Department of Biochemical Engineering, University College London, Bernard Katz Building, London WC1E 6BT.

*Corresponding author Tel: +44 (0)20 7679 9582, Fax: +44 (0) 207 916 3943

Email: d.nesbeth@ucl.ac.uk

This article has been accepted for publication and undergone full peer review but has not been through the copyediting, typesetting, pagination and proofreading process which may lead to differences between this version and the Version of Record. Please cite this article as doi: 10.1002/btpr.2273

Received: Oct 29, 2015; Revised: Mar 14, 2016; Accepted: Apr 05, 2016

Abstract

Fab' fragments have become an established class of biotherapeutic over the last two decades. Likewise, developments in synthetic biology are providing ever more powerful techniques for designing bacterial genes, gene networks and entire genomes that can be used to the improve industrial performance of cells used for production of biotherapeutics. We have previously observed significant leakage of an exogenous therapeutic Fab' fragment into the growth medium during high cell density cultivation of an *Escherichia coli* production strain. In this study we sought to apply a promoter engineering strategy to address the issue of Fab' fragment leakage and its consequent bioprocess challenges. We used site directed mutagenesis to convert the P_{tac} promoter, present in the plasmid, pTTOD-A33 Fab', to a P_{tic} promoter which has been shown by others to direct expression at a 35% reduced rate compared to P_{tac}. We characterised the resultant production trains in which either P_{tic} or P_{tac} promoters direct Fab' fragment expression. The P_{tic} promoter strain showed a 25-30% reduction in Fab' expression relative to the original P_{tac} strain. Reduced Fab' leakage and increased viability over the course of a fed-batch fermentation were also observed for the P_{tic} promoter strain. We conclude that cell design steps such as the P_{tac} to P_{tic} promoter conversion reported here, can yield significant process benefit and understanding with respect to periplasmic Fab' fragment production. It remains an open question as to whether the influence of transgene expression on periplasmic retention is mediated by global metabolic burden effects or periplasm overcapacity.

Introduction

Mammalian proteins rarely achieve native folding when expressed exogenously in *E. coli*. This fact presents a particularly acute challenge for those seeking to harvest such proteins from *E. coli* for use as medicines. Typically, when mammalian transgenes are transcribed and translated in the *E. coli* cytosol nascent polypeptide chains bundle together in homoaggregates known as inclusion bodies (IBs). Such IBs require extensive bioprocess recovery steps before an active protein is obtained. A major factor that can drive IB formation in *E. coli* is the absence of the molecular machinery needed to perform mammalian post-translational modifications (PTM). In mammalian cells PTMs often involve incorporation of small molecule or carbohydrate moieties whose presence is necessary to achieve native folding. The absence of native folding then favours IB formation.

As well as their own misfolding, the overexpression of exogenous proteins by *E. coli* can also have deleterious global effects on the host cell. Activation of DNA distress 'SOS' response systems (1) and even apoptosis-like death (2,3) have been observed to occur as a direct result of the burdens caused by overexpression of exogenous proteins.

A number of approaches have emerged to reduce the overall expression level of exogenous proteins encoded by transgenes within recombinant plasmids, whilst at the same time maxmising recombinant protein yield and quality. Since the 1980s, plasmids whose origin of replication (ori) defines a high copy number have been a boon to molecular biology as they provide the high yields of plasmid DNA (pDNA) needed to facilitate DNA recombination procedures while having little physiological impact on cells grown in shake flasks. Meanwhile, low copy number plasmids have remained prevalent in industrial application because they tend to direct levels of transgene expression that are better tolerated by cells already pushed close to their metabolic limits by cultivation to high cell density in bioreactors. Choice of plasmid copy number for fine-tuning recombinant protein expression level is limited because, as yet, there is no library of oris with incrementally inreasing copy numbers. Instead only a small set of plasmid oris is avialable, with quite large steps in copy number

between oris, from 20 to 300 for instance. Typically, a given ori will direct a very broad range of copy number, from 300 to 500, depending on transgenes and host strain (30).

Another option for minimising metabolic burden on host cells is to avoid the classic setup whereby cells face an antibiotic challenge, which they must meet by expression of an exogenous antibiotic resistance gene present on a retained plasmid. Expression of such antibiotic resistance genes inevitably tends to contribute to the metabolic burden exerted by the plasmid. Antibiotic resistance transgenes can be replaced with an endogenous gene encoding a protein that performs an essential function within the host cell metabolism. Inactivation of the copy of the essential gene in the host cell genome makes retention of the plasmid essential for cell survival (31). For recombinant protein production, this 'auxotrophic complementation' approach thas shown promise at shake flask scale but investigations in bioreactors remain rare (32), as do studies at high cell density (OD_{600} > 100).

Biotechnologists designing plasmids for industrial production of recombinant proteins should consider both plasmid copy number and the selective pressure used to ensure plasmid retention. An additional design feature to consider is the choice of promoter uses to control transgene expression. Yakandawala et al. found that transgene expression with the strong T7 promoter resulted in up to 99.5% reduction in the abundance of certain *E. coli* housekeeping mRNA molecules through *MazEF* activation, whereas lower level expression driven by a T5 promoter caused no perturbation of host mRNAs (3). Interestingly, the *MazEF* endoribonuclease can be employed to down-regulate host cell protein production in order to simplify downstream processing and an expression system that exploits this function has been commercialised (4).

A common strategy for avoiding cytosolic IB formation and promoting correct folding of exogenous proteins is to genetically append them to short *E. coli* amino terminal peptides that signal transport to the periplasmic space (5). The process of translocation to the periplasm can even in some cases select for correct folding (6). Once inside the periplasm the oxidative environment enables disulphide bond formation and any subsequent folding events favoured by the presence of those bonds.

In addition to periplasmic targeting, many researchers have attempted to balance the level of transgene expression driven by transgenic promoters with the global capacity of the host cell to replicate DNA, transcribe DNA to RNA, translate RNA to protein and translocate protein across membranes (33). Such balancing, or harmonisation, of promoter strength can be critical for efficient translocation of periplasm-targeted proteins. Excessive expression leads to crowding of transolocons, the transport machineries that mediate transport back and forth between the cytosol and periplasm. This in turn can lead to translocation failure and inclusion body formation (7). Options to address these issues include decreasing transgene translation rate (8), choosing alternative trafficking pathways to exploit (9,10) and employing *MazEF* activation to globally downregulate expression of those host cell proteins native to the periplasm and outer membrane that constitute a competing load on the capacity of translocons (11).

Balancing promoter strength with the overall metabolic burden of cellular 'housekeeping' processes could allow also address translocon overload caused by periplasmic translocation of exogenous proteins. In this way promoter engineering can be used to indirectly remodel trafficking events. In elegant work with two different recobinant proteins trafficked to the periplasm via the same route, Schlegel et al. showed that gene expression above a certain threshold can saturate the Sec-translocon capacity (33). Promoter engineering has been employed by synthetic biologists to improve biofuel production (12), optimise synthetic gene network performance (13) and enable construction of novel genetic logic gates (14). For instance, engineering the promoters encoded by a plasmid to control expression of an antibiotic resistance marker and the lacI repressor resulted in a four-fold increase in recombinant protein production at shake flask scale (15).

The tools and approaches developed in synthetic biology, such as genome refactoring (16), represent a potentially powerful new route to improved industrially relevant scale performance by harmonising promoter design with engineering application. Song et al. (17) provide a notable example where they developed a bacterial strain for production of 3-aminopropionic acid (3APA). Firstly they refactored a multi-gene locus from

Corynebacterium glutamicum (C. glutamicum) which includes the *panD* gene for an L-aspartate-α-decarboxylase. All the native *C. glutamicum* promoters within this locus were substituted with defined and designed synthetic promoters to enhance control and minimize epistatic cross talk and feedback effects. Finally the engineered locus was ported *en bloc* into an *E. coli* strain previously modified to produce fumaric acid. The final, engineered strain achieved yields of 32.3 g/L 3APA in fed-batch fermentation (17). Similarly, in the yeast *Pichia pastoris*, the highest ever yield of 18 g/L of active, secreted, recombinant cellulase to date was achieved by integrating the design of the cell cultivation programme and the design of the promoter used to control transgene expression (18).

For the workhorse strain of the biotechnology industry, *E. coli*, the most commonly utilised promoters were originally designed and assembled using genetic elements from the T7 bacteriophage and elements native to *E. coli* such as the P_{lac} and P_{trp} promoters (19, 20) and the *lac* operon. The resultant synthetic promoters, such as P_{tac} and P_{trc} , are highly active when de-repressed by the presence of isopropyl β-D-1-thiogalactopyranoside (IPTG). P_{trc} differs from P_{tac} by only a single base insertion between bases at the -10 and -35 positions relative to the start codon (20). This alteration impacts the interaction between the -10 and -35 sites and RNA polymerase and subsequent transcription. The expression dynamics arising from another P_{tac} variant, the P_{tic} promoter, have been characterised using shake flask cultivation by Brosius et al. (20) who determined its activity to be 65% of the parental P_{tac} promoter.

In this study we seek to address the upstream bioprocess consequences that arise from using a highly active promoter, P_{tac}, to drive expression of a therapeutic Fab' fragment in the periplasmic space. We previously (21) observed leakage of Fab' into the cell exterior after 20-30 hours of P_{tac} induction. As such we were keen to ascertain if this leakage occurs as a consequence of Fab' expression level. Our approach is to mutagenise the P_{tac} promoter to convert it to a P_{tic} promoter that has been shown by others to drive lower levels of transcription.

Bäcklund et al. (22) observed that post-induction glycerol feed rate can influence leakage of a recombinant Fab' from *E. coli* cells during 5-8 L bioreactor cultivation in a minimal salt medium. This suggests that the metabolic status of the cell may also play a significant role in its ability to maintain the integrity of the outer membrane during overexpression of exogenous proteins. To shed some light on this we used a flow cytometry approach to determine, at different stages of cultivation, the proportion of cells that are healthy and those that are non-viable (dead or dying) and have punctured outer membranes.

We use an industrial protocol for cultivation of cells to high cell density and induction of periplasmic Fab' expression using a 7.5 L bioreactor and defined media (21) to compare performance of cells in which Fab' expression is driven either by the P_{tac} or P_{tic} promoters. We also attempt to determine the point of leakage as a function of the predicted percentage occupation of periplasm volume.

Materials and Methods

All chemicals were purchased from Sigma Chemical Co. Ltd. (Dorset, UK), unless stated otherwise, and were of analytical grade.

Promoter engineering

The plasmid pTODDA33 (UCB, Brussels, Belgium) encodes a therapeutic Fab' fragment under the control of a P_{tac} promoter. The P_{tac} promoter was converted into the P_{tic} promoter described by Brosius et al. (20) by insertion of one cytosine and one guanine base between the -10 and -35 regions to extend the spacing by two residues. Forward and reverse primers of sequence GCTGTTGACAATTAATCATCGCGGCTCGTATAATGTGTGGAA and TTCCACACATTATACGAGCCGCGATGATTAATTGTCAACAGC respectively were used to introduce the mutation following the Stratagene QuikChange™ site directed mutagenesis protocol. Plasmids were transformed into the *E. coli* W3110 strain using standard molecular biology techniques (23).

Fed-batch fermentation and Fab' fragment quantitation

The Balasundaram et al. (24) cell cultivation protocol was linearly scaled down for use in New Brunswick BioFlo 110 7.5 L bioreactors. Samples were centrifuged to pellet cells and supernatant was decanted into a separate vessel and both pellet and supernatant were stored overnight (16-20 hours) at -20^{o}C before Fab' quantitation. The Nesbeth et al. (21) procedure was used to assay total and extracellular dimeric Fab' concentrations by protein G HPLC.

PIX staining and flow cytometry

Flow cytometry was performed using an Accuri C6 flow cytometer (BD Biosciences, USA) with bis-oxonol (BOX) and propidium iodide (PI) stains (PIX). Analysis using this method has been described by others (25) as an accurate method to measure cell viability (ability to exclude BOX) and permeability (PI uptake). Briefly, fermentation samples were diluted to an OD_{600} of 1.0 and 10 µL combined with 990 µL of a staining solution consisting of 5 µg/mL bis-oxonol, 4 mM ethylenediaminetetraacetic acid (EDTA), 2 µg/mL propidium iodide, in phosphate-buffered saline (PBS). Samples were stained for 8 minutes before analysis. Appropriate compensation was applied to correct for spectral overlap between the stains with the BD Accuri C6 software package, and results were gated to exclude cellular and other debris. Cells that remained unstained by BOX were counted to provide an overall measurement of viable cells/mL; cells which were stained by BOX and PI were counted to provide permeable cells/mL measurement. Differences caused by changing biomass levels were accounted for by reporting cells per mL per OD_{600} unit, as previously performed by Volkmer et al. (26). Any readings displaying just PI staining were attributed to cell fragments and other debris, and discounted from calculations.

Mathematical modelling of periplasm occupancy

Concentration of dimer obtained by HPLC analysis was converted into units per cell by using Equation 1 and assuming 100% conversion of monomer to correctly folded dimer, with a predicted dimer weight of $8.4E10^{-17}$ mg/unit and volume of $6.06E10^{-23}$ L/unit. The total volume of the periplasm is assumed to be $6.5E10^{-17}$ L (27).

$$\frac{Fab'concentration}{cell\ concentration\ \times Fab'weight} \times \frac{V_{Fab'}}{V_P} \times 100\% = Percentage\ occupancy$$

Equation 1. Calculation of percentage periplasm occupancy from Fab' concentration (mg/L); cell concentration (cells/L), Fab' weight (mg/unit), volume of Fab' fragment (L/unit), and volume of periplasm (L).

Results and Discussion

Conversion of P_{tac} to P_{tic}

The addition of two bases, cytosine and a guanine, between the -10 and -35 sites of the P_{tac} promoter (Figure 1) generates the P_{tic} promoter which was characterised previously at shake flask scale with respect to its ability to direct expression of chloramphenicol acetyltransferase and *E. coli* 4.5 S RNA (17). In that study the P_{tic} promoter showed a 35% decrease in expression compared to the parental P_{tac} promoter when used to express the same ORFs. Here we used site directed mutagenesis (SDM) to effect the P_{tac} to P_{tic} conversion within the pTODD A33 plasmid (21) upstream of the Fab' fragment heavy and light chain open reading frames (ORFs). The insertion mutation was confirmed by sequencing and the P_{tic}-pTODD A33 plasmid was transformed into the *E. coli w3110* production strain to produce the *Fabi* strain. The original P_{tac}-pTODD A33 plasmid was also transformed into *w3110* to produce the *Fab* strain.

Growth and productivity impacts of P_{tac} to P_{tic} conversion

Fermentations were performed according to previously described protocols (24), scaled for use in a 7.5 L bioreactor. The *Fab* and *Fabi* strains showed similar growth profiles (Figure 2), with differences in OD_{600} attributable to the 20% variation expected between fermentation runs (21). For the *Fab* strain OD_{600} began to decrease at 88 hours post-inoculation, which is 48 hours post-induction. OD_{600} of the *Fabi* strain decreased 88 hours post-inoculation, 48 hours post-induction (Figure 2). We interpreted the decrease in OD_{600} as the onset of cell disintegration and death. Total and external Fab' levels were measured using protein G HPLC as previously described (21, 22), and these values used to calculate the internal

(Figure 3A) and external (Figure 3B) levels of Fab' accumulation. Internal Fab' fragment accumulation occurs at a 25-30% slower rate (Figure 3A) for the *Fabi* strain (0.23 mg Fab' / g cell weight / hour) compared to the *Fab* strain (0.32 mg Fab' / g cell weight/ hour). In Figure 3B the level of external Fab' is plotted over both the entire 60 hour post-induction period (larger graph) and the first 40 hours only (inset graph). In this post-induction, pre-death period external Fab' fragment levels represent 5 – 8 % of total protein (internal and external) for the *Fabi* strain and 10 – 23% for the *Fab* strain over three experimental repeats. Despite the fact that a greater proportion of Fab' fragment has leaked to the cell exterior for the *Fab* strain, the periplasmic filling profile for both strains is similar (Figure 3C), apart from the final time point in which periplasmic Fab' levels appear apparently decreased.

Percentage periplasm filling was calculated as described in Equation 1, and both strains show a similar increase over time, never exceeding 7%. Moreover, cell populations for both strains reach the onset of lysis at 48 hours post induction, when percentage occupancy exceeds 6%. This suggests that the maximum space available within the periplasm for recombinant protein synthesis is approximately 6% and that beyond this point leakage of periplasm contents to the cell exterior is triggered.

Impeller speed suggests less cell death events with P_{tic} promoter compared to P_{tac}

A number of different mechanisms may explain the appearance of Fab' fragment in the growth medium. When over 6% of total periplasm volume is occupied by exogenous protein, the outer membrane may rupture in a manner that is fatal to the cell. Alternatively, a pathway may exist whereby cells overexpressing exogenous periplasmic Fab' fragment can 'vent' Fab' periplasmic contents to the cell exterior in order to counteract the production surplus. Theoretically such controlled periplasmic venting (CPV) could be triggered directly by detection of internal Fab' levels exceeding a 6% threshold of total periplasmic volume. Alternatively, exceeding the 6% threshold may be purely coincidental and CPV could in fact be triggered by other factors, such as metabolic burden or unfolded protein response. Notwithstanding the triggering mechanism, we sought to differentiate between periplasmic rupture and CPV using a selection of experiments.

Firstly we attempted to determine the level of cell death that occurs during bioreactor cultivation of each strain. For many microbial fermentation processes, including *E. coli*, impeller speed correlates to the oxygenation requirement of a given culture (28). In the fermentation protocol used here (21), cells are maintained in carbon-limited idiophasic growth post-induction resulting in markedly less oxygen demand than trophophase growth. Any significant increase in the viscosity of the cell suspension would not be due to cell growth, see post-induction turbidity in Figure 2, would hinder oxygen transfer and thus would trigger increased impeller speed due to the operation of proportional-integral-differential (PID) algorithms within the bioreactor control unit.

When *E. coli* cells die during high cell density cultivation the released intracellular contents, particularly the high molecular weight heteropolymeric DNA genome, tend to significantly increase the viscosity of the cell suspension through aggregation and other processes (29). As no process other than cell growth or release of cell contents is believed to impact viscosity, any significant increases in post-induction process stream viscosity can be regarded as an indicator of the level of cell contents release, i.e. cell death. Therefore impeller speed can in this context be considered as an indirect indicator of cell death.

Post-induction impeller speed during bioreactor cultivation of each strain is plotted in Figure 4. Immediately after induction both *Fab* and *Fabi* strains show a rapid drop in impeller speed, which is expected due to the downshift in oxygen demand characteristic of transition from trophophase to carbon-limited, idiophasic growth. For the *Fabi* strain, impeller speed then remains relatively constant until the final stage of the fermentation, 45-50 hours post-induction when OD_{600} drops indicating that a large proportion of cells are undergoing disintegration and death (Figure 4). By contrast, for the *Fab* strain impeller speed steadily increases from approximately 10 hours post induction until the maximum attainable speed is reached. Maximal impeller speed triggers pure oxygen gas blending to maintain the 30% dissolved oxygen tension (DOT) set point (Figure 4). This scenario, of maximal impeller speed plus gas blending, persists until the drop in OD_{600} at 45-50 hours post-induction.

These impeller speed profiles suggest a greater number of cell death events occur during *Fab* strain cultivation compared to the *Fabi* strain. This observation is consistent with the greater levels of Fab' leakage observed with the Fab strain being due to lethal outer membrane punctures occurring as a result of periplasm overcapacity.

Differential stain uptake indicates greater cell viability with P_{tic} promoter compared to P_{tac}

To test if Fab' leakage results from lethal outer membrane rupture events we used a flow cytometry staining method to calculate the precise number of healthy cells and non-viable, permeabilised cells present at different stages of the fermentation. Lewis et al. (25) previously, investigating batch fermentation of *E. coli* in a 5L bioreactor, used bis-oxonol (BOX) binding to differentiate between healthy *E. coli* cells with intact, therefore polarised membranes, that do not bind BOX, and cells with de-polarised outer membranes, a marker of cell stress, that do bind BOX. In the same study Lewis et al. (25) also used propidium iodide (PI) uptake to stain only cells with permeabilised outer membrane. In this way BOX plus PI (PIX) analysis by flow cytometry can be used to determine how many cell present in a given sample are health, stressed or dead and permeabilised.

In Figure 5 samples taken at the indicated time points were incubated with PIX and analysed by flow cytometry. For each sample analysed by flow cytometry and the number of unstained cell and stained cell detection events were logged and then divided by the OD_{600} of the sample in accordance with a procedure performed previously by Volkmer et al. (26). The profile of viable cell numbers is mirrored between *Fabi* and *Fab* strains, with the difference in absolute numbers falling within the variation observed between repeat fermentation runs (Figure 5A). After accounting for inter-experiment variation, the *Fab* strain cultivation still produces a far greater number of dead, permeabilised cells compared to the *Fabi* strain (Figure 5B). More than double the number of dead permeable cells is observed in *Fab* strain cultivation compared to the *Fabi* strain for most time points post induction.

The ratio of healthy, stressed and permeabilised cells at different stages of the fermentation is can also be visualised in the plots of PIX staining in Figure 6. Cultures of both strains

consist of approximately 97% healthy cells just prior to induction (Figure 6A and 6B, 0 hours post-induction). However, after 35 hours of induction the *Fab* strain showed a greater proportion of stressed (7.1% BOX-only stained) cells (Figure 6) compared to the *Fabi* strain (4.6% BOX-only stained). 35 hours post-induction the proportion of dead, permeablilised cells (6.6%) measured for the *Fab* strain was over double that of the *Fabi* strain (3.1%). This ratio persisted to a degree even at the end of fermentation, when OD_{600} is dropping, with 18.1% and 11.6% of *Fab* strain and *Fabi* strain cells, respectively, being dead and permeabilised.

Conclusions

We successfully established the P_{tic} promoter in the pTTOD-A33 Fab' fragment expression plasmid by mutagenesis of the original P_{tac} promoter (Figure 1), generating the *Fabi* strain and the parental *Fab* strains respectively. Growth performance of the strains was comparable in a 7.5 L bioreactor using an industrial cultivation protocol (Figure 2). Conversion of P_{tac} to P_{tic} resulted in a 25-35% decrease in Fab' fragment expression rate (Figure 3A), which is comparable to the 35% decrease observed by Brosius et al. (20). Relative to the *Fab* parental strain, decreased intracellular accumulation of Fab' fragment in the *Fabi* strain was accompanied by decreased appearance of Fab' fragment in the surrounding growth media over the first 40 hours of induction (Figure 3B). This is despite almost identical predicted rates of periplasmic filling (Figure 3C). In a previous study (21) with the *Fab* strain we observed that cell debris may sequester Fab' fragment during centrifugation steps in a manner that involves released genomic DNA (Figure 6 of that study). We suspect the large proportion of permeabilised cells observed here (Figure 5B) may be contributing to the lower than expected level of internal Fab' measured 55 hours post-induction (Figure 3A) and the consequently low level of periplasm occupation by Fab' predicted in the final time point of Figure 3C.

Indirect evidence, from impeller speed profiles (Figure 4) and PIX staining (Figures 5 and 6), indicated that the elevated Fab' fragment levels in growth media observed in the first 40

hours post-induction for the parental *Fab* strain are likely due to an increased prevalence of dead cells in which the integrity and function of the outer membrane have been compromised. We conclude that decreasing Fab' expression by promoter engineering results in a decreased cytotoxic burden on the cell, while maintaining growth and productivity performance.

We anticipate that future experiments may establish whether the cytotoxic burdens associated with P_{tac}-drived Fab' expression are a cause or consequence of the periplasm reaching overcapacity. The mechanism of this cytotoxicity is also currently unknown. HPLC data gathered during this study and the studies of Balasundaram et al. (24) and Nesbeth et al. (21) did not indicate the presence of any significant level of non-dimer or non-monomer Fab' in cell lysates. More direct approaches, such as gel filtration or dynamic light scattering (DLS) could better establish the level, if any, of IB-formation for the expressed Fab' fragment. A cytsol-targetted version of the Fab' fragment in this study could also be used to dissect the role of periplasm overcapacity versus global metabolic burden in causing cell stress. In the wider context of production and application of antibody-based proteins, we suggest a broad palette of cell engineering options should always be considered, such as engineered cytosolic disulphide bridge formation (34), plasmid copy number choice, antibody-free plasmid retention and promoter engineering.

Figure Legends

Figure 1. P_{tac} and P_{tic} promoters. Schematic representation of P_{tac} and P_{tic} promoters (panel A), and specific base insertions (panel B). The P_{tic} insertion was made by site directed mutagenesis and increases the gap between the -10 and -35 sites by two bases (underlined).

Figure 2. Growth of *Fabi* and *Fab* strains in 7.5 L fed-batch fermentation. Seed trains were prepared by inoculating 200 mL selective LB media in a 1 L shake flask with a single, 600 µL working cell bank stock. This culture was grown until an OD_{600} of 1.0 was reached, where a 40 mL aliquot was removed and used to inoculate 360 mL selective defined media. This culture was then grown to an OD_{600} of 5.0, then used to inoculate 3.4 L of defined media without antibiotic in a 7.5 L bioreactor, giving a final volume of 4 L and starting OD_{600} of 0.75. A previously described protocol (24) was scaled for use at this scale. Error bars indicate standard deviation over n=3 measurements.

Figure 3. Intracellular, extracellular and periplasmic accumulation of Fab' fragment. At the end of trophophasic growth cells were induced by addition of 10 mL 15.31 g/L IPTG, and then fed 80% glycerol at a rate of 6.4 mL/hour until fermentation end. Following the previously described protocol (21), post induction Fab' production was measured by protein G HPLC, and extracellular and total Fab' levels were measured to allow the calculation of intracellular Fab'. Intracellular Fab' levels were plotted in graph A. Extracellular Fab' levels were plotted for 60 hours post induction (graph B, larger graph) and only the first 40 hours (graph B, inlaid graph). Percentage of total periplasm volume predicted by Equation 1 to be occupied by Fab' was plotted in graph C. Data sets shown are indicative of n=3 measurements. Error bars indicate standard deviation over n=3 measurements which was <5% for all data points so error bars fall within marker symbols.

Figure 4. Post induction impeller speed and gas blending. Impeller speeds and gas mixing post induction are plotted. A target level of 30% dissolved oxygen tension was set for the bioreactor control unit.

Figure 5. Physiological status of cells post-induction. Unstained cell and stained cell detection events in a given sample were divided by the OD_{600} of the sample in accordance with a procedure performed previously by Volkmer et al. (26). Error bars indicate standard deviation over n=2 measurements.

Figure 6. Cellular PIX staining profiles post-induction. Post induction PI / BOX (PIX) staining profiles, as measured by flow cytometry, of *Fab* (A) and *Fabi* (B) strains after zero, 35 and 54 hours post-induction. For each profile the lower left quadrant is gated as zero PIX staining and indicates healthy cells. Staining with PI only (upper left quadrant) is attributed to fragments and other debris. Staining with BOX only (lower right quadrant) indicates cells undergoing stress and cells stained with both BOX and PI (upper right quadrant) are both non-viable (dead/dying) and permeabilised. Data sets shown are indicative of n=2 measurements.

Acknowledgements

Support from the EPSRC and BJS Biotechnologies is gratefully acknowledged.

References

1. Arís A, Corchero JL, Benito A, Carbonell X, Viaplana E, Villaverde A. The expression of recombinant genes from bacteriophage lambda strong promoters triggers the SOS response in Escherichia coli. Biotechnol Bioeng. 1998 Dec 5;60(5):551–9.

2. Erental A, Sharon I, Engelberg-Kulka H. Two Programmed Cell Death Systems in Escherichia coli: An Apoptotic-Like Death Is Inhibited by the mazEF-Mediated Death Pathway. Rosenberg SM, editor. PLoS Biol. 2012 Mar 6;10(3):e1001281.
3. Yakandawala N, Gawande PV, LoVetri K, Romeo T, Kaplan JB, Madhyastha S. Enhanced expression of engineered ACA-less beta-1, 6-N-acetylglucosaminidase (dispersin B) in Escherichia coli. J Ind Microbiol Biotechnol. 2009 Oct;36(10):1297–305.
4. Suzuki M, Mao L, Inouye M. Single protein production (SPP) system in Escherichia coli. Nat Protoc. 2007;2(7):1802–10.
5. Dammeyer T, Tinnefeld P. Engineered fluorescent proteins illuminate the bacterial periplasm. Comput Struct Biotechnol J. 2012 Nov 22;3:e201210013. doi: 10.5936/csbj.201210013. eCollection 2012.
6. Robinson C, Matos CF, Beck D, Ren C, Lawrence J, Vasisht N, Mendel S. Transport and proofreading of proteins by the twin-arginine translocation (Tat) system in bacteria. Biochim Biophys Acta. 2011 Mar;1808(3):876-84. doi: 10.1016/j.bbamem.2010.11.023. Epub 2010 Nov 29.
7. de Marco A. Recombinant polypeptide production in E. coli: towards a rational approach to improve the yields of functional proteins. Microb Cell Factories. 2013;12(1):101.
8. Gupta P, Lee KH. Silent mutations result in HlyA hypersecretion by reducing intracellular HlyA protein aggregates. Biotechnol Bioeng. 2008 Dec 1;101(5):967–74.
9. Sletta H, Nedal A, Aune TEV, Hellebust H, Hakvåg S, Aune R, et al. Broad-host-range plasmid pJB658 can be used for industrial-level production of a secreted host-toxic single-chain antibody fragment in Escherichia coli. Appl Environ Microbiol. 2004 Dec;70(12):7033–9.
10. Sletta H, Tondervik A, Hakvag S, Aune TEV, Nedal A, Aune R, et al. The Presence of N-Terminal Secretion Signal Sequences Leads to Strong Stimulation of the Total Expression Levels of Three Tested Medically Important Proteins during High-Cell-

Density Cultivations of Escherichia coli. Appl Environ Microbiol. 2006 Dec 1;73(3):906–12.

11. Samuelson JC. Recent developments in difficult protein expression: a guide to E. coli strains, promoters, and relevant host mutations. Methods Mol Biol Clifton NJ. 2011;705:195–209.
12. Atsumi S, Hanai T, Liao JC. Non-fermentative pathways for synthesis of branched-chain higher alcohols as biofuels. Nature. 2008 Jan 3;451(7174):86–9.
13. Arpino JAJ, Hancock EJ, Anderson J, Barahona M, Stan G-BV, Papachristodoulou A, et al. Tuning the dials of Synthetic Biology. Microbiology. 2013 Jul 1;159(Pt_7):1236–53.
14. Cox RS, Surette MG, Elowitz MB. Programming gene expression with combinatorial promoters. Mol Syst Biol. 2007;3:145.
15. Pasini M, Fernández-Castané A, Jaramillo A, de Mas C, Caminal G, Ferrer P. Using promoter libraries to reduce metabolic burden due to plasmid-encoded proteins in recombinant Escherichia coli. New Biotechnol. 2015 Aug 31;
16. Leon Y Chan, Sriram Kosuri, and Drew Endy. Refactoring bacteriophage T7. Molecular Systems Biology (2005) doi:10.1038/msb4100025.
17. Song CW, Lee J, Ko Y-S, Lee SY. Metabolic engineering of Escherichia coli for the production of 3-aminopropionic acid. Metab Eng. 2015 Jul;30:121–9.
18. Mellitzer A, Ruth C, Gustafsson C, Welch M, Birner-Grünberger R, Weis R, et al. Synergistic modular promoter and gene optimization to push cellulase secretion by Pichia pastoris beyond existing benchmarks. J Biotechnol. 2014 Dec 10;191:187–95.
19. de Boer HA, Comstock LJ, Vasser M. The tac promoter: a functional hybrid derived from the trp and lac promoters. Proc Natl Acad Sci U S A. 1983 Jan;80(1):21–5.
20. Brosius J, Erfle M, Storella J. Spacing of the -10 and -35 regions in the tac promoter. Effect on its in vivo activity. J Biol Chem. 1985 Mar 25;260(6):3539–41.

21. Nesbeth DN, Perez-Pardo M-A, Ali S, Ward J, Keshavarz-Moore E. Growth and productivity impacts of periplasmic nuclease expression in an Escherichia coli Fab' fragment production strain. Biotechnol Bioeng. 2012.
22. Bäcklund E, Reeks D, Markland K, Weir N, Bowering L, Larsson G. Fedbatch design for periplasmic product retention in Escherichia coli. J Biotechnol. 2008 Jul 31;135(4):358–65.
23. Green MR, Sambrook J, Sambrook J. Molecular cloning: a laboratory manual. 4th ed. Cold Spring Harbor, N.Y: Cold Spring Harbor Laboratory Press; 2012. 3 p.
24. Balasundaram B, Nesbeth D, Ward JM, Keshavarz-Moore E, Bracewell DG. Step change in the efficiency of centrifugation through cell engineering: co-expression of Staphylococcal nuclease to reduce the viscosity of the bioprocess feedstock. Biotechnol Bioeng. 2009 Sep 1;104(1):134–42.
25. Lewis G, Taylor I, Nienow A, Hewitt C. The application of multi-parameter flow cytometry to the study of recombinant Escherichia coli batch fermentation processes. J Ind Microbiol Biotechnol [Internet]. 2004 Jul 13 [cited 2013 Oct 14];31(7). Available from: http://link.springer.com/10.1007/s10295-004-0151-8
26. Volkmer, B., Heinemann, M., 2011. Condition-Dependent Cell Volume and Concentration of *Escherichia coli* to Facilitate Data Conversion for Systems Biology Modeling. PLoS ONE 6, e23126. doi:10.1371/journal.pone.0023126
27. Sundararaj S. The CyberCell Database (CCDB): a comprehensive, self-updating, relational database to coordinate and facilitate in silico modeling of Escherichia coli. Nucleic Acids Res. 2004 Jan 1;32(90001):293D – 295.
28. Doran PM. Bioprocess Engineering Principles [Internet]. Academic Press; 1995. 439 p. Available from: http://www.sciencedirect.com/science/book/9780122208553
29. Kong S, Day AF, O'Kennedy RD, Shamlou PA, Titchener-Hooker NJ. Using viscosity-time plots of *Escherichia coli* cells undergoing chemical lysis to measure the impact of physiological changes occurring during batch cell growth. J Chem Technol Biotechnol. 2009 May;84(5):696–701.

30. Ford T et al. Plasmids 101: A Desktop Resource. 2015 October. Addgene. Available from: http://info.addgene.org/download-addgenes-ebook-plasmids-101-1st-edition.

31. Dong W-R, Xiang L-X, Shao J-Z. Novel Antibiotic-Free Plasmid Selection System Based on Complementation of Host Auxotrophy in the NAD De Novo Synthesis Pathway. Aprilr. Appl. & Env. Microb. 2010 April:2295-2303.

32. Selvamani RSV, Telaar M, Friehs K and Flaschel E. Antibiotic-free segregational plasmid stabilization in Escherichia coli owing to the knockout of triosephosphate isomerase (tpiA). 2014 Microbial Cell Factories, 13:58.

33. Schlegel S, Rujas E, Ytterberg AJ, Zubarev RA, Luirink J, de Gier J-W. Optimizing heterologous protein production in the periplasm of *E. coli* by regulating gene expression levels. 2013 Microbial Cell Factories, 12:24.

34. de Marco A. Recombinant antibody production evolves into multiple options aimed at yielding reagents suitable for application-specific needs. 2015 Microbial Cell Factories, 14:125.

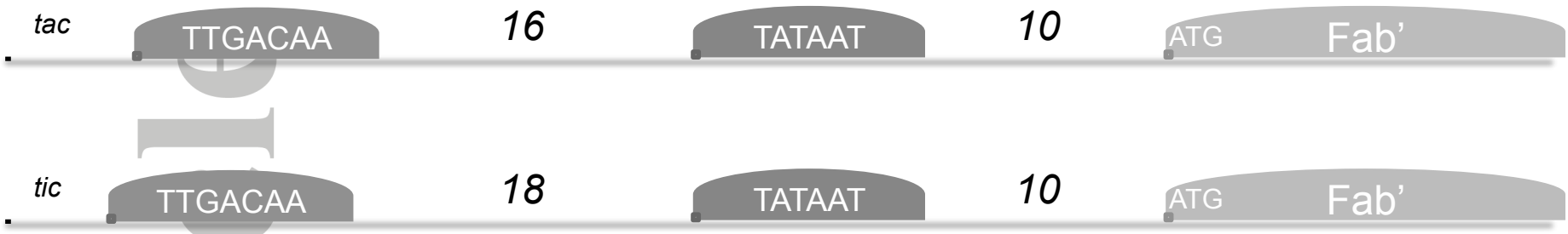

-35 -10

P_{tac} TTGACAATTAATCAT--CGGCTCGTATAATGTGTGGAA

-37 -10

P_{tic} TTGACAATTAATCATCCGGCTCGTATAATGTGTGGAA

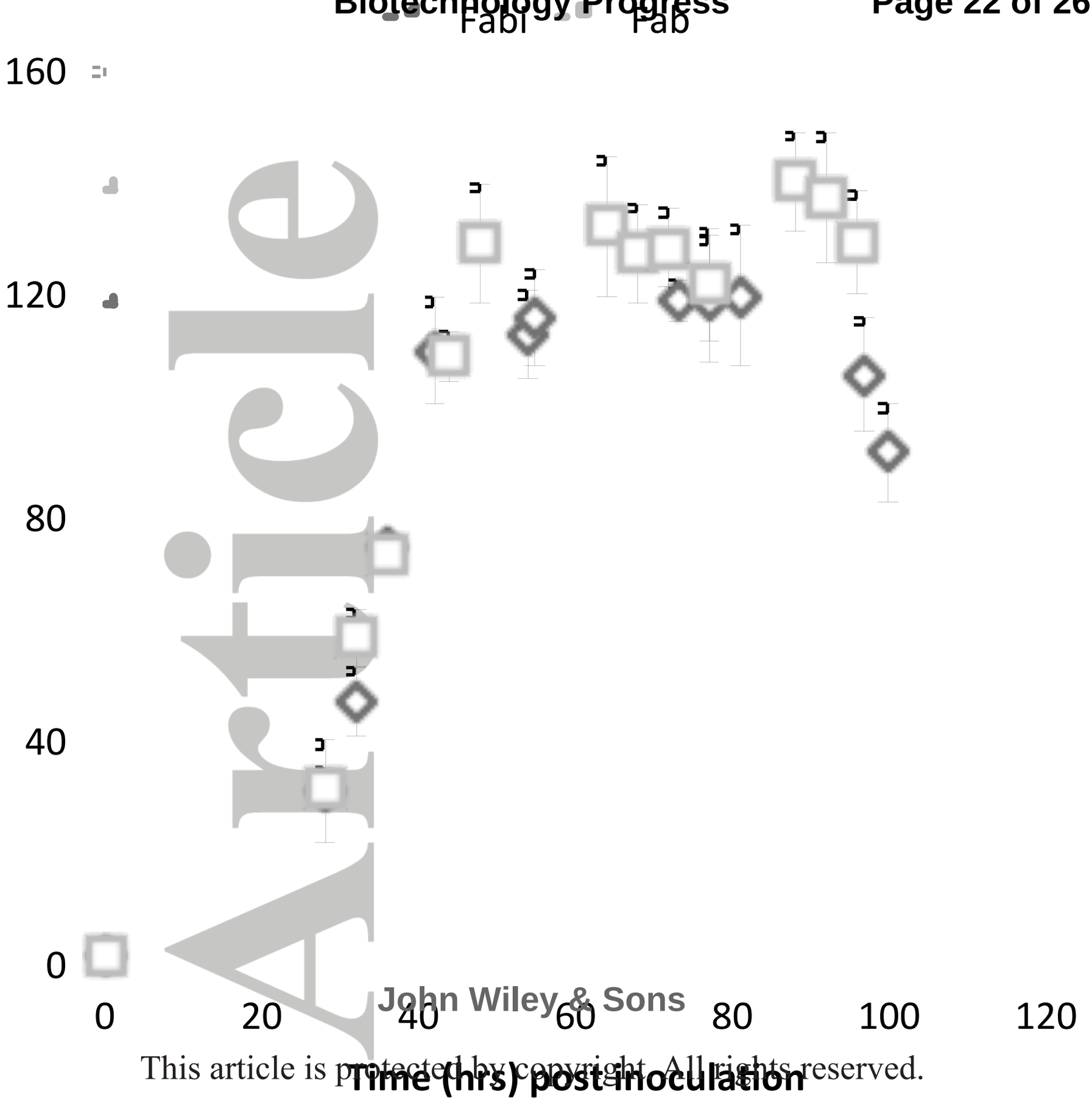

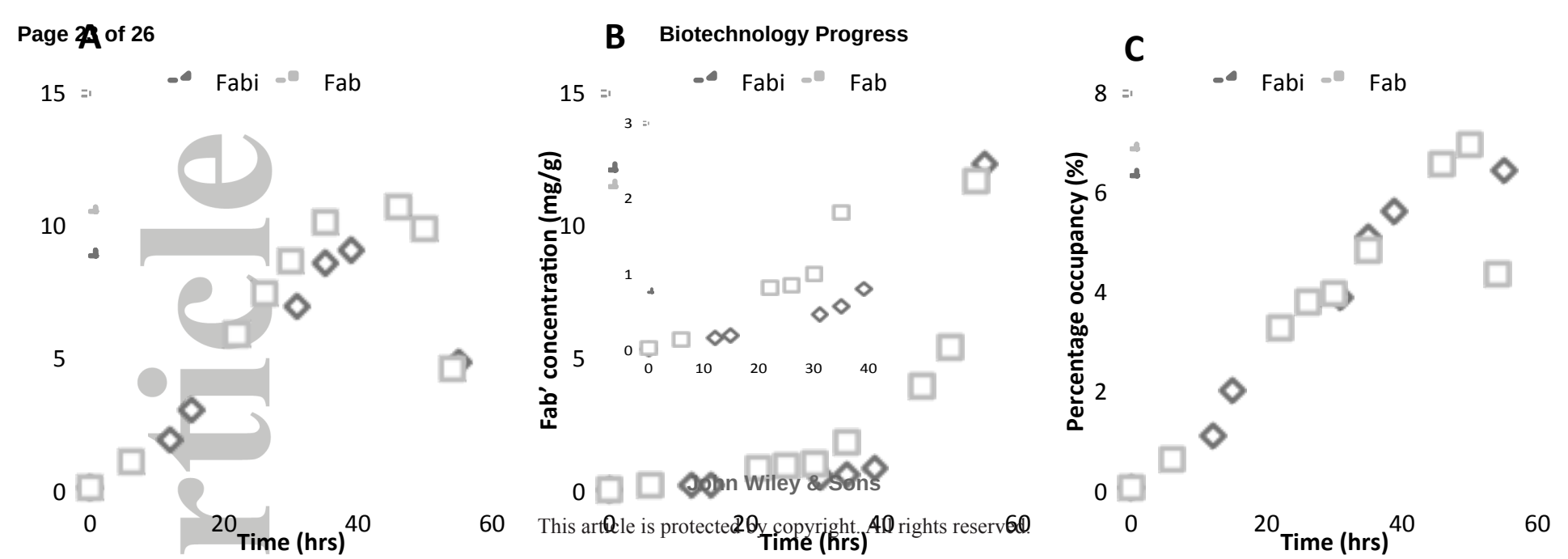

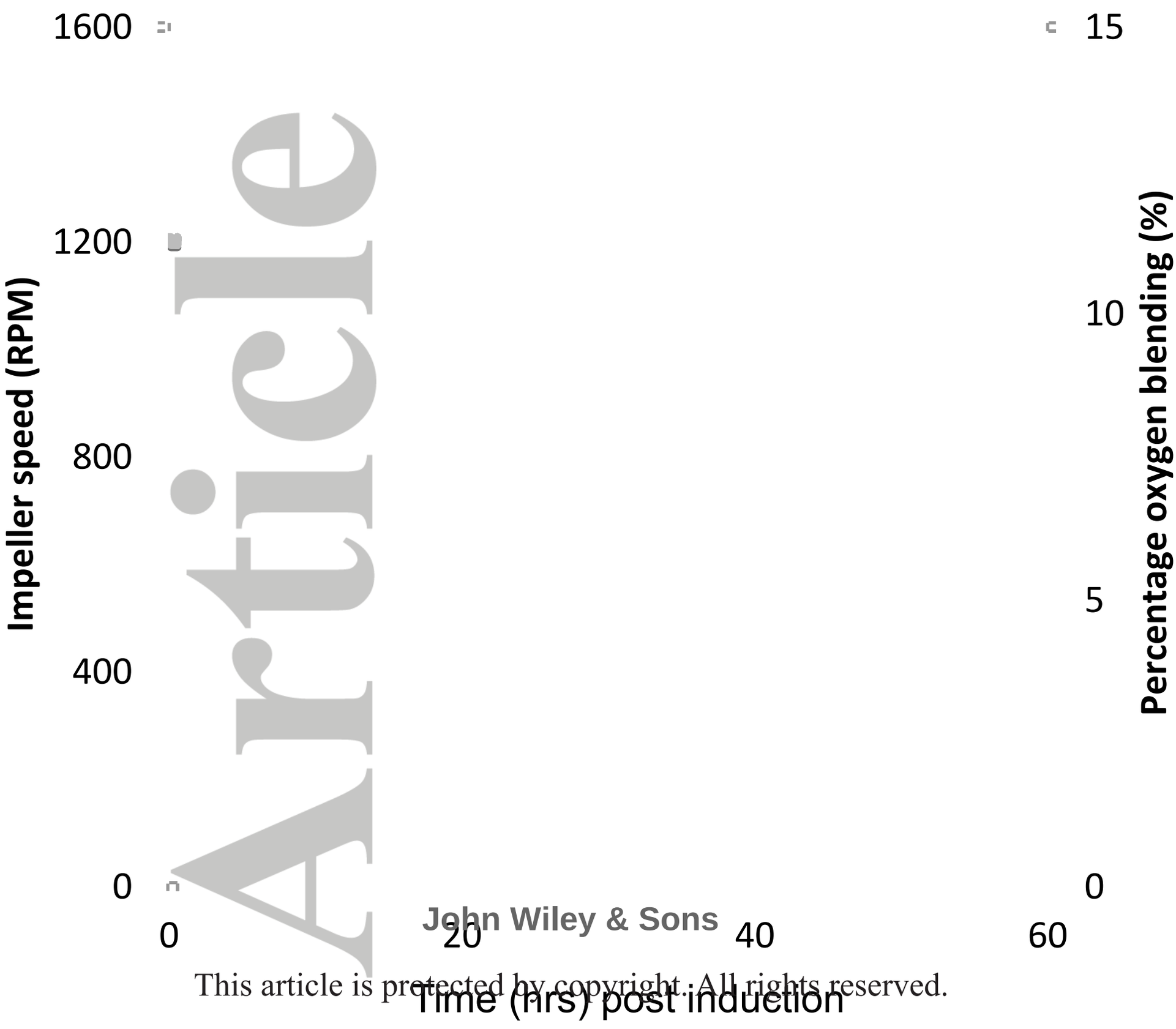

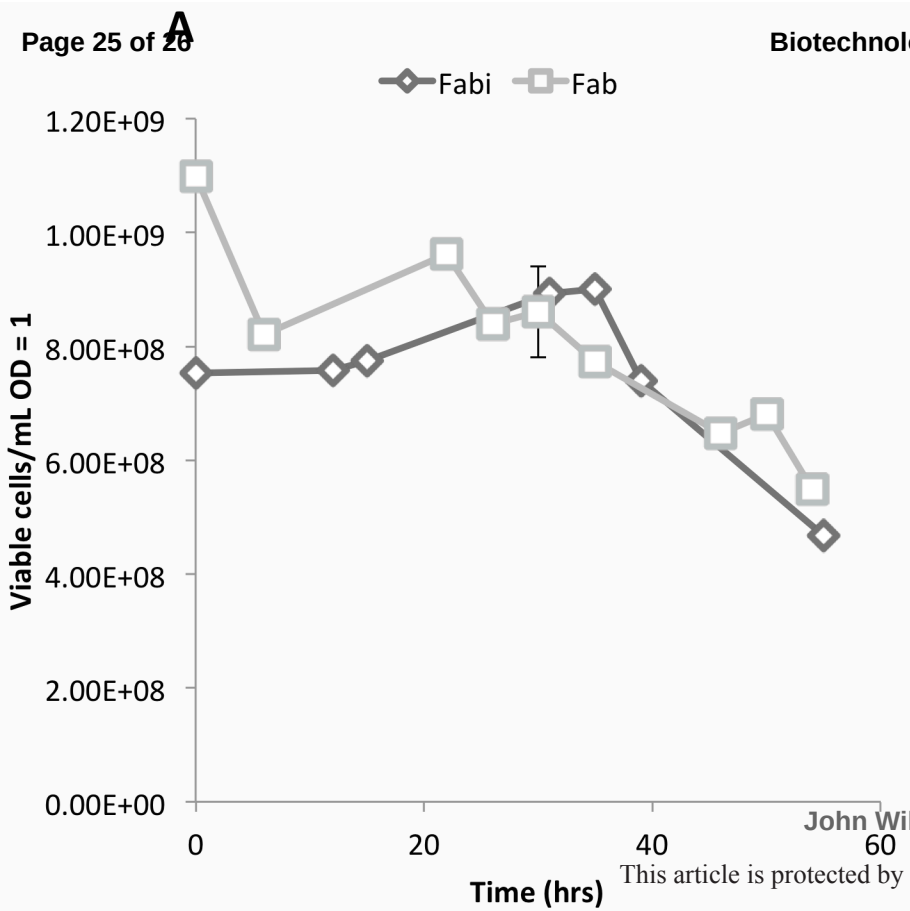

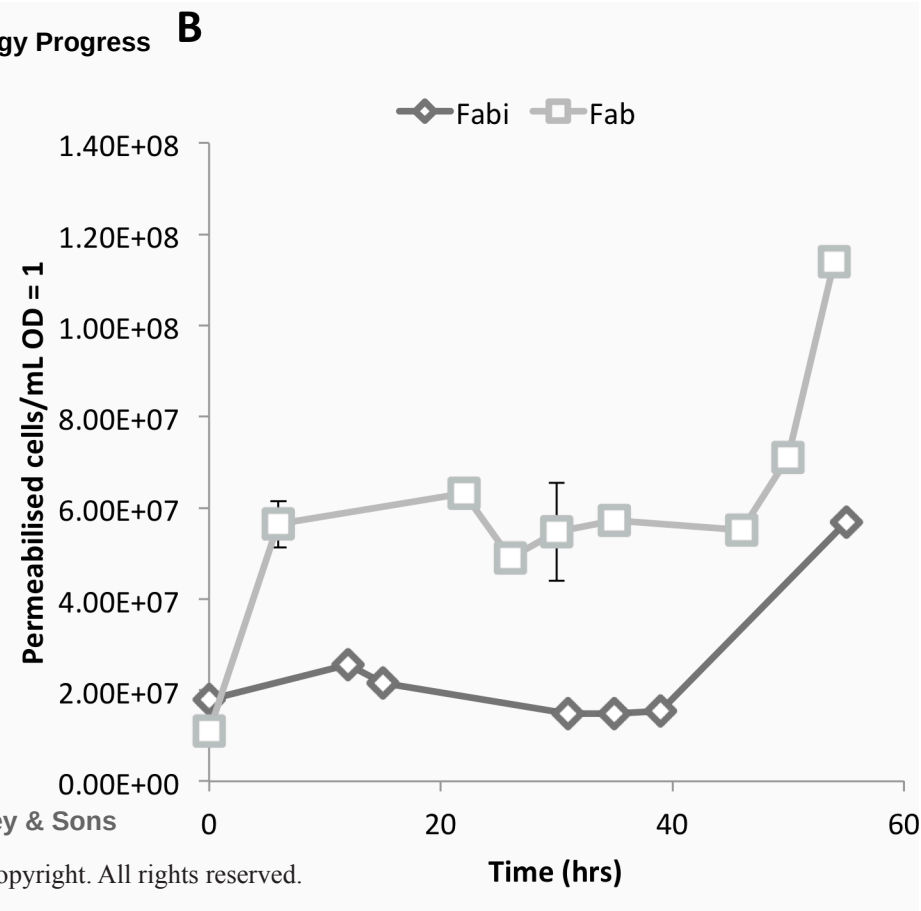

Time (hrs)
Post-Induction

0 35 54

PI Staining

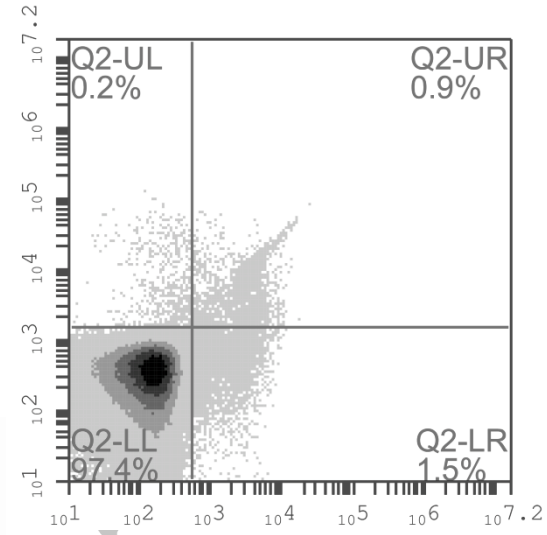

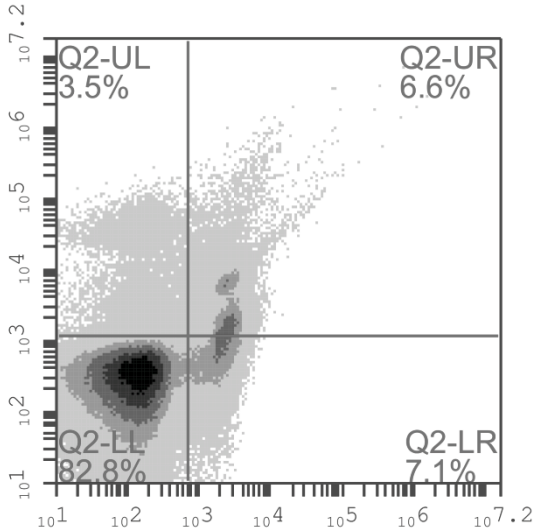

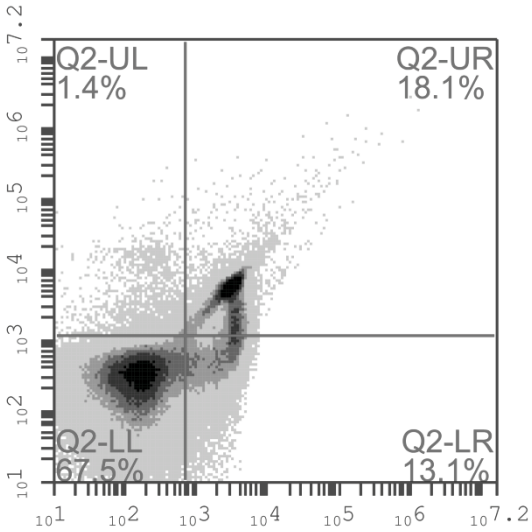

B

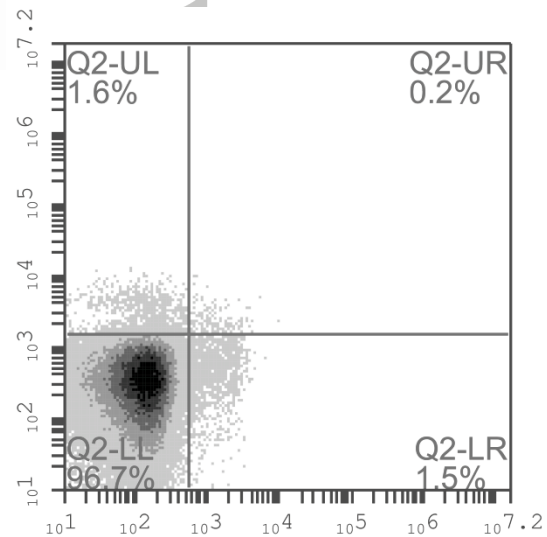

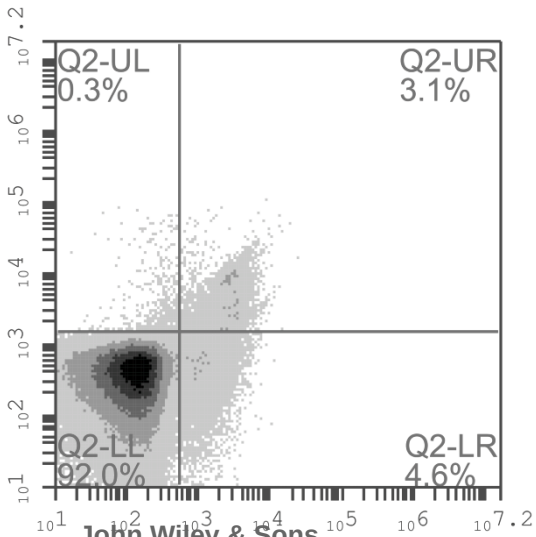

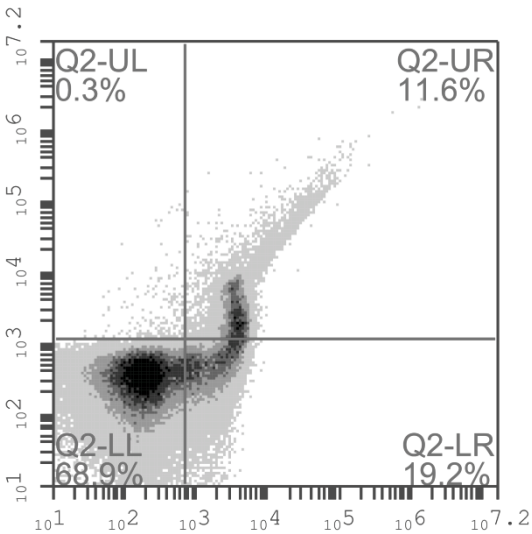

BOX Staining